IEEE Access
Multidisciplinary | Rapid Review | Open Access Journal

Received January 21, 2019, accepted January 28, 2019, date of publication February 1, 2019, date of current version February 20, 2019.

Digital Object Identifier 10.1109/ACCESS.2019.2896979

Direction-of-Arrival Estimation for Both Uncorrelated and Coherent Signals in Coprime Array

HAIYUN XU, DAMING WANG, BIN BA, WEIJIA CUI, AND YANKUI ZHANG
National Digital Switching System Engineering and Technological Research Center, Zhengzhou 450001, China

Corresponding author: Bin Ba (xidianbabin@163.com)

This work was supported in part by the National Natural Science Foundation of China, under Grant 61401513.

ABSTRACT Direction-of-arrival (DOA) estimation in coprime array involves the problem that there is the coexistence of both uncorrelated signals and coherent signals in the multipath environment. An approach to estimate DOA of uncorrelated and coherent signals separately, based on the coprime linear array and coprime planar array, is proposed in this paper. The uncorrelated signals are estimated first, where the root multiple signal classification (root-MUSIC) is applied in the coprime linear array and unitary estimating signal parameters via rotational invariance techniques (Unitary-ESPRIT) is utilized in the coprime planar array. Those subspace algorithms are of low complexity compared with the spectral peak search method. We then eliminate the components of noises and uncorrelated signals and reconstruct a covariance matrix of coherent signals. Finally, we use the root-MUSIC or Unitary-ESPRIT to resolve the one-dimensional or two-dimensional DOAs of coherent signals, respectively. The simulation results demonstrate the computational efficiency and high accuracy of the proposed algorithm. The results also prove that this algorithm can estimate the number of signals more than that of subarray sensors and separate two signals from the same angle.

INDEX TERMS Direction-of-arrival, coprime linear array, coprime planar array, coherent signals.

I. INTRODUCTION

Direction-of-arrival (DOA) estimation for multiple uncorrelated signals is a fundamental task in many applications such as radar [1], underwater acoustics [2], [3], indoor navigation, and wireless communication [4]. In most researches, the uniform non-sparse arrays, such as uniform linear array and uniform rectangular array (URAs) [5], with subspace algorithms can obtain high-resolution DOA estimations. The multiple signal classification (MUSIC) [6] is a spectral peak search method. However, it owns large computational complexity. The root-MUSIC [7], estimating signal parameters via rotational invariance techniques (ESPRIT) [8], propagation method (PM) [9], and Unitary-ESPRIT [10], [11] aim to reduce the complexity efficiently. The algorithms mentioned above are all based on uncorrelated signals. However, there are usually the coherent signals or highly correlated signals in multipath environment, which results in the low rank of signals subspace. Thus, the subspace algorithms become invalid to estimate DOAs for coherent signals and highly correlated signals. In uniform non-sparse array, spatial smoothing divides an array into multiple overlapping subarrays, and combines all covariance matrices of subarrays to recovery the rank of the signals subspace [12], [13]. Besides spatial smoothing, in uniform non-sparse array, a processing that estimates the DOAs of uncorrelated signals and coherent signals, separately, has a favorable performance [14]–[17]. The methods are all based on the processing that estimates the uncorrelated signals, then eliminates the components of them, and resolves the coherent signals at last. Thus, they can estimate the number of signals more than that of sensors.

Nowadays, the coprime arrays, a kind of sparse array, including coprime linear arrays [18]–[20] and coprime planar arrays [21], [22], which are respectively applied to estimate one-dimensional (1D) and two-dimensional (2D) DOAs, have become a focus. Compared with a uniform non-sparse array, a coprime array has a larger aperture with the same number of sensors so that it can acquire a higher accuracy. When the signals are coherent, the coprime array can also have effective methods. We consider that the coprime array consists of two uniform arrays, then we respectively use spatial smoothing in each subarray, and apply common

The associate editor coordinating the review of this manuscript and approving it for publication was Yue Zhang.

peak search method to find the real DOAs [20]–[22]. Unfortunately, one disadvantage of spatial smoothing is that it reduces the maximum number of signals resolved. Moreover, common peak search also limits the number of signals resolved less than that of subarray sensors. Hence, if we combine those two methods to estimate coherent signals in coprime array, we will not be able to estimate multiple signals with limited sensors. Two active estimation algorithms in coprime linear array of multiple-input multiple-output (MIMO) system have been presented in [23] and [24]. But the active detection has a higher cost than passive detection. A passive estimation method in coprime linear array uses fourth-order cumulants matrix (FCM), which can estimate the number of signals more than that of sensors, but it needs another supplementary sparse array [25].

In this paper, we introduce the methods from [15] and [17] to coprime model to estimate both coherent and uncorrelated signals, where we consider both coprime linear array and coprime planar array. We present the algorithms steps and prove that the methods in uniform non-sparse array can also be applied to sparse array. Compared with spatial smoothing in coprime array, we can estimate the number of signals bigger than that of subarray sensors. Compared with the existing passive estimation algorithms, we need no supplementary array in coprime linear array. Moreover, we have made some improvements to reduce the complexity. We use root-MUSIC in coprime linear array. Partial spectral search (PSS) [21] and 2D-ESPRIT [22] have been utilized in coprime planar array, where the former is still based on spectral peak finding and the latter needs to match parameters. Hence, we utilize Unitary-ESPRIT in coprime planar array, which obtain the lowest complexity than PSS and 2D-ESPRIT without parameters matching.

The paper is organized as follows. We first present two array models in Section 2. In Section 3, we explain our approach to estimate DOAs, and show the steps of the proposed algorithm. The computational complexity and the maximum number of signals resolved analysis are presented in Section 4. In Section 5, we show the results of simulations. Finally, we summarize work in Section 6. Throughout this paper, $\mathbf{I}_N$ represents the N dimensional unit array; $(\bullet)^T$, $(\bullet)^*$ and $(\bullet)^H$ respectively represent the transposition, conjugation and conjugate transposition; *diag* $[\bullet]$ represents a vector transforming to a diagonal matrix; $\otimes$ denotes the Kronecker product; $\lceil\bullet\rceil$ denotes the round up to the number.

II. SYSTEM MODEL

Considering the coprime array model, 1D and 2D array geometry are shown in Fig. 1 and 2, respectively. 1D coprime array is generally made up of two uniform linear arrays. Subarray 1 has M_1 sensors and subarray 2 has M_2 sensors, where M_1 and M_2 are the coprime integers (generally assuming $M_1 < M_2$). We define the mth sensor location of the ith ($i = 1, 2$) subarray as $(m-1)M_{\bar{i}}\lambda/2$ ($\bar{i} = 1, 2$ *and* $\bar{i} \neq i$), where λ denotes the wavelength. Hence, the steering vector

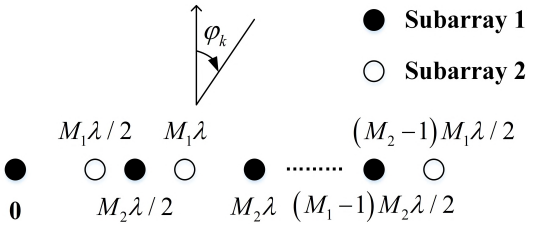

FIGURE 1. Geometry of coprime linear array.

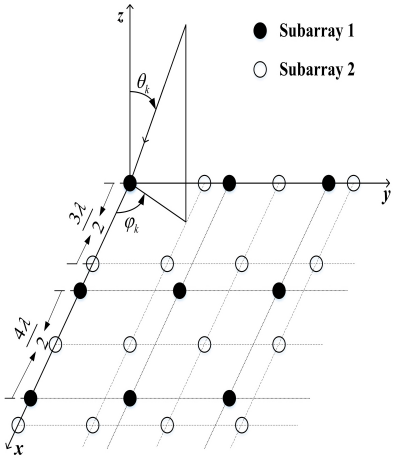

FIGURE 2. Geometry of coprime planar array when $M_1 = 3$, $M_2 = 4$.

of coprime linear array is given by

$$\mathbf{a}_i(\varphi) = \left[1, e^{-j\pi M_{\bar{i}}\sin\varphi}, \cdots, e^{-j\pi(M_i-1)M_{\bar{i}}\sin\varphi}\right]^T, \quad (1)$$

where φ is the DOA of one signal. As for 2D coprime array, we combine two uniform rectangular arrays, where subarray 1 has $M_1 \times M_1$ sensors and subarray 2 has $M_2 \times M_2$ sensors, and the space distance between the two adjacent sensors is $M_{\bar{i}}\lambda/2$. The steering vector of coprime planar array is denoted as

$$\mathbf{b}_i(\varphi, \theta) = \mathbf{a}_{y_i} \otimes \mathbf{a}_{x_i}, \quad (2)$$

where

$$\mathbf{a}_{x_i}(\varphi, \theta) = \left[1, e^{-j\pi M_{\bar{i}}\sin\theta\cos\varphi}, \cdots, e^{-j\pi(M_i-1)M_{\bar{i}}\sin\theta\cos\varphi}\right]^T, \quad (3)$$

$$\mathbf{a}_{y_i}(\varphi, \theta) = \left[1, e^{-j\pi M_{\bar{i}}\sin\theta\sin\varphi}, \cdots, e^{-j\pi(M_i-1)M_{\bar{i}}\sin\theta\sin\varphi}\right]^T, \quad (4)$$

and (φ, θ) are the azimuth angle and elevation angle of one signal, respectively.

Suppose that there are K narrowband far-field signals impinging on the array. Assume P coherent signal groups, where the pth group has L_p signals. The coherent signal coming from $\varphi_{p,\ell}$ or $(\varphi_{p,\ell}, \theta_{p,\ell})$ is corresponding to the ℓth multipath propagation of $S_p(t)$ with power σ_p^2 for $p = 1, \cdots, P$. The signals within each group are coherent to each other and uncorrelated to those in the different group. The total number

of coherent signals is $K_c = \sum_{p=1}^{P} L_p$. And the remaining signals, $S_k(t)$ coming from φ_k or (φ_k, θ_k) with the power σ_k^2 for $k = K_c + 1, \cdots, K$, are uncorrelated to each other. The number of those signals is $K_u = K - K_c$. Thus, the received signals at the ith subarray can be represented as

$$\begin{aligned}\mathbf{X}_i^{(1)}(t) &= \sum_{p=1}^{P}\sum_{\ell=1}^{L_p}\mathbf{a}_i\left(\varphi_{p,\ell}\right)\beta_{p,\ell}S_p(t) \\ &\quad + \sum_{k=K_c+1}^{K}\mathbf{a}_i(\varphi_k)S_k(t) + \mathbf{n}_i^{(1)}(t) \\ &= \mathbf{A}_i\mathbf{S}(t) + \mathbf{n}_i^{(1)}(t), \qquad (5)\\ \mathbf{X}_i^{(2)}(t) &= \sum_{p=1}^{P}\sum_{\ell=1}^{L_p}\mathbf{b}_i\left(\varphi_{p,\ell},\theta_{p,\ell}\right)\beta_{p,\ell}S_p(t) \\ &\quad + \sum_{k=K_c+1}^{K}\mathbf{b}_i(\varphi_k,\theta_k)S_k(t) + \mathbf{n}_i^{(2)}(t) \\ &= \mathbf{B}_i\mathbf{S}(t) + \mathbf{n}_i^{(2)}(t), \qquad (6)\end{aligned}$$

where the array manifold matrices are denoted as

$$\mathbf{A}_i(\varphi) = [\mathbf{a}_i(\varphi_1)\ \cdots\ \mathbf{a}_i(\varphi_K)], \qquad (7)$$

$$\mathbf{B}_i(\varphi,\theta) = [\mathbf{b}_i(\varphi_1,\theta_1)\ \cdots\ \mathbf{b}_i(\varphi_K,\theta_K)], \qquad (8)$$

and $\beta_{p,\ell}$ is the complex fading coefficient of the ℓth coherent signals in the pth group. The signal data vector

$$\mathbf{S}(t) = \left[\beta_{1,1}S_1(t), \cdots, s_K(t)\right]^T, \qquad (9)$$

where $t = 1, \cdots, J$ is sampling time and J is the number of snapshots. And the noise vector is usually Gaussian random variables with zero means and variance σ_n^2.

III. DOA ESTIMATION FOR BOTH UNCORRELATED AND COHERENT SIGNALS

From (5) and (6), we can obtain the received signal covariance matrix of the ith ($i = 1, 2$) subarray as

$$\mathbf{R}_{\mathbf{X}_i}^{(1)} = \frac{1}{J}\mathbf{X}_i^{(1)}\mathbf{X}_i^{(1)H} = \mathbf{A}_i\mathbf{R}_\mathbf{S}\mathbf{A}_i^H + \sigma_n^2\mathbf{I}_{M_i}, \qquad (10)$$

$$\mathbf{R}_{\mathbf{X}_i}^{(2)} = \frac{1}{J}\mathbf{X}_i^{(2)}\mathbf{X}_i^{(2)H} = \mathbf{B}_i\mathbf{R}_\mathbf{S}\mathbf{B}_i^H + \sigma_n^2\mathbf{I}_{M_i^2}, \qquad (11)$$

where $\mathbf{R}_\mathbf{S} = \mathbf{S}\mathbf{S}^H/J$. If there exist the coherent signals, the rank of $\mathbf{R}_\mathbf{S}$ is $P + K_u$, which is smaller than K. The conventional spatial smoothing is used to increase rank of signal subspace to K. However, The algorithms in [15] and [17] divide covariance matrix into two parts, according to uncorrelated and coherent signals, and just needs to enhance the rank of covariance matrix of coherent signals to K_c. In coprime array, the processing of algorithms is changed and shown in following parts.

A. DOA ESTIMATION FOR UNCORRELATED SIGNALS

Generally, the MUSIC and 2D-MUSIC can be applied to find DOAs in linear array and rectangular array, respectively. However, to reduce the complexity burden, we apply root-MUSIC [7] and Unitary-ESPRIT [10] to solve this problem.

In coprime linear array, through root-MUSIC, we can get the estimation $\hat{\varphi}_{i,k}$ ($k = K_c + 1, \cdots, K$). But because the space between the adjacent sensors is more than half wavelength, the $\hat{\varphi}_{i,k}$ may be an ambiguous value. If we get the one possible value of one signal, we can solute all possible values, including the real value, by the relationship between ambiguous values and real value. The relationship is given by

$$M_{\bar{i}}\sin\varphi_{i,real} = 2m + M_{\bar{i}}\sin\varphi_{i,ambiguous} \quad (-M_{\bar{i}} \le m \le M_{\bar{i}}). \qquad (12)$$

Then we define the two sets as

$$\Phi_{i,k}^{(1)} = \{\hat{\varphi}_{i,k,m} | \hat{\varphi}_{i,k,m} = \arcsin(\sin\hat{\varphi}_{i,k} + 2m/M_{\bar{i}})\} \quad (-M_{\bar{i}} \le m \le M_{\bar{i}}), \qquad (13)$$

$$\Phi_i^{(1)} = \{\Phi_{i,K_c+1}^{(1)}, \cdots, \Phi_{i,K}^{(1)}\}. \qquad (14)$$

Through finding the common values between the set $\Phi_{2,k}$ and Φ_1, we can obtain the real DOA estimation $\hat{\varphi}_k^r$ of the uncorrelated signal.

Similarly, as for coprime planar array, the possible estimation $(\hat{\varphi}_{i,k}, \hat{\theta}_{i,k})$ can be resolved via Unitary-ESPRIT. Consider the relationship between ambiguous values and real value, which is represented as (15), as shown at the top of the next page. Thus, we can also have corresponding sets given by (16) and (17), shown at the top of the next page.

Through finding the common values between the set $\Phi_{2,k}^{(2)}$ and $\Phi_1^{(2)}$, and $\Theta_{2,k}^{(2)}$ and $\Theta_1^{(2)}$, we can calculate the real values $\hat{\mu}_k^r$ and $\hat{\nu}_k^r$. Furthermore, the DOA estimation $(\hat{\varphi}_k^r, \hat{\theta}_k^r)$ $(k = K_c + 1, \cdots, K)$ is denotes as

$$\begin{cases}\hat{\theta}_k^r = \arcsin\left(\sqrt{\left(\hat{\mu}_k^r\right)^2 + \left(\hat{\nu}_k^r\right)^2}\right) \\ \hat{\varphi}_k^r = \arctan\left(\hat{\nu}_k^r/\hat{\mu}_k^r\right).\end{cases} \qquad (18)$$

B. DOA ESTIMATION FOR COHERENT SIGNALS

1) ELIMINATE THE COMPONENTS OF NOISES AND UNCORRELATED SIGNALS

We first eliminate the components of the noises, following the steps as:

$$\mathbf{R}_i^{(1)} = \hat{\mathbf{R}}_{\mathbf{X}_i}^{(1)} - \hat{\sigma}_{n_i}^2\mathbf{I}_{M_i} \approx \mathbf{A}_i\mathbf{R}_\mathbf{S}\mathbf{A}_i^H, \qquad (19)$$

$$\mathbf{R}_i^{(2)} = \hat{\mathbf{R}}_{\mathbf{X}_i}^{(2)} - \hat{\sigma}_{n_i}^2\mathbf{I}_{M_i^2} \approx \mathbf{B}_i\mathbf{R}_\mathbf{S}\mathbf{B}_i^H, \qquad (20)$$

where $\hat{\sigma}_{n_i}^2$ is the average value of $M_i - K_u - P$ smallest eigenvalues of $\hat{\mathbf{R}}_{\mathbf{X}_i}^{(1)}$ or $M_i^2 - K_u - P$ smallest eigenvalues of $\hat{\mathbf{R}}_{\mathbf{X}_i}^{(2)}$. Moreover, the $\mathbf{R}_\mathbf{S}$ can be rewritten as

$$\mathbf{R}_\mathbf{S} = \begin{bmatrix}\mathbf{R}_{\mathbf{S}_1} & & & & \\ & \ddots & & & \\ & & \mathbf{R}_{\mathbf{S}_{K_c}} & & \\ & & & \sigma_{K_c+1}^2 & \\ & & & & \ddots \\ & & & & & \sigma_K^2\end{bmatrix}, \qquad (21)$$

$$\begin{cases} M_{\bar{i}} \sin\theta_{i,real} \cos\varphi_{i,real} = 2m_x + M_{\bar{i}} \sin\theta_{i,ambiguous} \cos\varphi_{i,ambiguous} \ (-M_{\bar{i}} \le m_x \le M_{\bar{i}}) \\ M_{\bar{i}} \sin\theta_{i,real} \sin\varphi_{i,real} = 2m_y + M_{\bar{i}} \sin\theta_{i,ambiguous} \sin\varphi_{i,ambiguous} \ (-M_{\bar{i}} \le m_y \le M_{\bar{i}}) \end{cases} \tag{15}$$

$$\begin{cases} \Phi_{i,k}^{(2)} = \{\hat{\mu}_{i,k,m_x} | \hat{\mu}_{i,k,m_x} = 2m_x/M_{\bar{i}} + \sin\hat{\theta}_{i,k} \cos\hat{\varphi}_{i,k}, -M_{\bar{i}} \le m_x \le M_{\bar{i}}\} \\ \Theta_{i,k}^{(2)} = \{\hat{\nu}_{i,k,m_y} | \hat{\nu}_{i,k,m_y} = 2m_y/M_{\bar{i}} + \sin\hat{\theta}_{i,k} \sin\hat{\varphi}_{i,k}, -M_{\bar{i}} \le m_y \le M_{\bar{i}}\} \end{cases} \tag{16}$$

$$\begin{cases} \Phi_{i}^{(2)} = \{\Phi_{i,K_c+1}^{(2)}, \cdots, \Phi_{i,K}^{(2)}\} \\ \Theta_{i}^{(2)} = \{\Theta_{i,K_c+1}^{(2)}, \cdots, \Theta_{i,K}^{(2)}\} \end{cases} \tag{17}$$

$$R_i^{(1)}(m,n) = \sum_{p=1}^{P} \sum_{\ell=1}^{L_p} \sigma_p^2 \beta_{p,\ell}^* \gamma_p^m e^{j\pi(n-1)M_{\bar{i}} \sin\varphi_{p,\ell}} + \sum_{k=K_c+1}^{K} \sigma_k^2 e^{j\pi(n-m)M_{\bar{i}} \sin\varphi_k} \tag{23}$$

$$r_i^{(1)}(m,n) = R_i^{(1)}(m,n) - R_i^{(1)*}(M_i - m + 1, M_i - n + 1) \tag{25}$$

$$\begin{aligned} R_i^{(2)}(m_x, m_y, n_x, n_y) &= \sum_{p=1}^{P} \sum_{\ell=1}^{L_p} \sigma_p^2 \beta_{p,\ell}^* \eta_p^{m_x,m_y} e^{j\pi M_{\bar{i}} \sin\theta_{p,\ell}((n_x-1)\cos\varphi_{p,\ell} + (n_y-1)\sin\varphi_{p,\ell})} \\ &\quad + \sum_{k=K_c+1}^{K} \sigma_k^2 e^{j\pi M_{\bar{i}} \sin\theta_k((n_x-m_x)\cos\varphi_k + (n_y-m_y)\sin\varphi_k)} \end{aligned} \tag{28}$$

$$\eta_p^{m_x,m_y} = \sum_{\ell'=1}^{L_p} \beta_{p,l'} e^{j\pi M_{\bar{i}} \sin\theta_{p,\ell'}\left((1-m_x)\cos\varphi_{p,\ell'} + (1-m_y)\sin\varphi_{p,\ell'}\right)} \tag{29}$$

$$r_i^{(2)}(m_x, m_y, n_x, n_y) = R_i^{(2)}(m_x, m_y, n_x, n_y) - R_i^{(2)*}(M_i - m_x + 1, M_i - m_y + 1, M_i - n_x + 1, M_i - n_y + 1) \tag{30}$$

$$r_i^{(2)}(m_x, m_y, n_x, n_y) = \sum_{p=1}^{P} \sum_{\ell=1}^{L_p} \sigma_p^2 \zeta_{p,l}^{m_x,m_y} e^{j\pi M_{\bar{i}} \sin\theta_{p,\ell}((n_x-1)\cos\varphi_{p,\ell} + (n_y-1)\sin\varphi_{p,\ell})} \tag{31}$$

$$\zeta_{p,\ell}^{m_x,m_y} = \sum\nolimits_{\ell'=1}^{L_p} \left(\beta_{p,\ell}^* \beta_{p,\ell'} - \beta_{p,\ell} \beta_{p,\ell'}^*\right) e^{j\pi M_{\bar{i}} \sin\theta_{p,\ell'}\left((1-m_x)\cos\varphi_{p,\ell'} + (1-m_y)\sin\varphi_{p,\ell'}\right)} \tag{32}$$

where

$$\begin{aligned} \mathbf{R}_{\mathbf{S}_p} &= \frac{1}{J} \begin{bmatrix} \beta_{p,1}\mathbf{S}_1 \\ \vdots \\ \beta_{p,L_p}\mathbf{S}_p \end{bmatrix} \begin{bmatrix} \beta_{p,1}^* \mathbf{S}_1^H & \cdots & \beta_{p,L_p}^* \mathbf{S}_p^H \end{bmatrix} \\ &= \begin{bmatrix} \beta_{p,1}\beta_{p,1}^* & \beta_{p,1}\beta_{p,2}^* & \cdots & \beta_{p,1}\beta_{p,L_p}^* \\ \beta_{p,2}\beta_{p,1}^* & \beta_{p,2}\beta_{p,2}^* & \cdots & \beta_{p,2}\beta_{p,L_p}^* \\ \vdots & \vdots & \vdots & \vdots \\ \beta_{p,L_p}\beta_{p,1}^* & \beta_{p,L_p}\beta_{p,2}^* & \cdots & \beta_{p,L_p}\beta_{p,L_p}^* \end{bmatrix} \sigma_p^2. \end{aligned} \tag{22}$$

Thus, the element of $\mathbf{R}_i^{(1)}$ in the mth row and nth column is expressed as (23), shown at the top of this page, where $\gamma_p^m = \sum_{\ell'=1}^{L_p} \beta_{p,\ell'} e^{j\pi(1-m)M_{\bar{i}} \sin\varphi_{p,\ell'}}$. Because the covariance matrix of uncorrelated signals is a Hermite matrix, we can get the relationship between the uncorrelated signals component of $R_i^{(1)}(m,n)$ and that of $R_i^{(1)*}(M_i - m + 1, M_i - n + 1)$ as

$$\begin{aligned} &\sum_{k=K_c+1}^{K} \sigma_k^2 e^{-j\pi((M_i-n+1)-(M_i-m+1))M_{\bar{i}} \sin\varphi_k} \\ &\qquad = \sum_{k=K_c+1}^{K} \sigma_k^2 e^{j\pi(\mathrm{n-m})M_{\bar{i}} \sin\varphi_k}, \end{aligned} \tag{24}$$

For $m, n = 1, \cdots, M_i$, we then define $r_i^{(1)}(m,n)$ as (25), shown at the top of this page, and $r_i^{(1)}(m,n)$ can be rewritten as

$$r_i^{(1)}(m,n) = \sum_{p=1}^{P} \sum_{\ell=1}^{L_p} \sigma_p^2 \xi_{p,\ell}^m e^{j\pi(n-1)M_{\bar{i}} \sin\varphi_{p,\ell}}, \tag{26}$$

where

$$\xi_{p,\ell}^m = \sum_{\ell'=1}^{L_p} \left(\beta_{p,\ell}^* \beta_{p,\ell'} - \beta_{p,\ell} \beta_{p,\ell'}^*\right) e^{j\pi(1-m)M_{\bar{i}} \sin\varphi_{p,\ell'}}. \tag{27}$$

Hence, we remove the components of uncorrelated signals via (25).

This processing can also be applied to the 2D symmetric rectangular array. The element of $\mathbf{R}_i^{(2)}$ in the $(M_i(m_x-1)+m_y)$th row and $(M_i(n_x-1)+n_y)$th column is denoted as (28), as shown at the top of the previous page, where $\eta_p^{m_x,m_y}$ is given by (29), shown at the top of the previous page. For $m_x, m_y, n_x, n_y = 1, \cdots, M_i$, we define the new value $r_i^{(2)}\left(m_x, m_y, n_x, n_y\right)$ as (30), shown at the top of the previous page, which can be rewritten as (31), as shown at the top of the previous page, where $\zeta_{p,\ell}^{m_x,m_y}$ is given by (32), shown at the top of the previous page. Thus, we eliminate the component of uncorrelated signals in coprime planar array via (30).

2) COHERENT SIGNALS IN COPRIME LINEAR ARRAY

In order to construct covariance matrix of coherent signals, whose rank is K_c, we utilize the feature that the covariance matrix of linear array is a Toeplitz matrix, and reconstruct a Toeplitz matrix based on $r_i^{(1)}(m,n)$. Define the new covariance matrix as

$$\begin{aligned}\mathbf{R}_{\mathbf{Y}_i}^{(1)}(m) &= \begin{bmatrix} r_i^{(1)}\left(m,\bar{M}_i\right) & \cdots & r_i^{(1)}(m,M_i) \\ \vdots & \vdots & \vdots \\ r_i^{(1)}(m,1) & \cdots & r_i^{(1)}(m,\bar{M}_i) \end{bmatrix} \\ &= \bar{\mathbf{A}}_i \boldsymbol{\Sigma}^{(1)}(m)\,\bar{\mathbf{A}}_i^H, \end{aligned} \tag{33}$$

where $\bar{M}_i = (M_i+1)/2$. If M_i is an even number, we just set $r_i^{(1)}\left(m,\bar{M}_i\right) = 0$. The new array manifold $\bar{\mathbf{A}}_i = \mathbf{J}\left[\mathbf{a}_i^*\left(\varphi_{1,1}\right), \cdots, \mathbf{a}_i^*\left(\varphi_{P,L_P}\right)\right]$, $\mathbf{J} = \left[\mathbf{O}_{\bar{M}_i\times(\bar{M}_i-1)}, \mathbf{I}_{\bar{M}_i}\right]$ and $\boldsymbol{\Sigma}^{(1)}(m) = \mathrm{diag}\left[\sigma_1^2\xi_{1,1}^m, \cdots, \sigma_P^2\xi_{P,L_P}^m\right]$. When $K_c < \bar{M}_i$, the rank of $\mathbf{R}_{\mathbf{Y}_i}^{(1)}$ is generally K_c.

As a result, we can apply root-MUSIC to $\mathbf{R}_{\mathbf{Y}_i}^{(1)}$ to solve the closed-form solutions of DOAs. Through (13) and (14), we can calculate all possible DOAs and find the common values $\hat{\varphi}_k^r$ $(k = 1, \cdots, K_c)$.

3) COHERENT SIGNALS IN COPRIME PLANAR ARRAY

In order to construct the covariance matrix of coherent signals based on a rectangular array, we first construct a new matrix $\mathbf{F}_{i,m_s}$ of size $M_{s1}^2 \times M_{s2}$ as (34), shown at the bottom of the next page, where $m_s = 1, \cdots, M_{s2}$ with $M_{s1}+M_{s2}-1 = M_i$, and $1 \le m_x, m_y \le M_i$. Arrange all $\mathbf{F}_{i,m_s}$ to a new matrix $\mathbf{F}_i$ as $\mathbf{F}_i = [\mathbf{F}_{i,1}, \cdots, \mathbf{F}_{i,M_{s2}}]$. Hence, construct the covariance matrix of coherent signals as

$$\mathbf{R}_{\mathbf{Y}_i}^{(2)} = \mathbf{F}_i\mathbf{F}_i^H. \tag{35}$$

When $M_{s2}^2 \ge K_c$ and $M_{s1}^2 > K_c$, the rank $\mathbf{R}_{\mathbf{Y}_i}^{(2)}$ is K_c, which satisfies the requirement of using Unitary-ESPRIT. We provide Theorem 1, the proof of which is postponed into Appendix A. And we can calculate $(\hat{\varphi}_k^r, \hat{\theta}_k^r)$ $(k = 1, \cdots, K_c)$ via (16),(17) and (18).

Theorem 1: If $M_{s2}^2 \ge K_c$ and $M_{s1}^2 > K_c$, the rank of $\mathbf{R}_{\mathbf{Y}_i}^{(2)}$ is K_c.

C. ALGORITHM STEPS CONCLUSION

The main steps for the proposed algorithms in coprime linear array and coprime planar array can be summarized as follows:

Algorithm 1 DOA Estimation Algorithm in Coprime Linear Array

1) Calculate the covariance matrix via (5) and estimate the DOAs of uncorrelated signals using root-MUSIC in each subarray.
2) Find the common values of two subarrays and obtain the real DOAs as $\hat{\varphi}_k^r$ $(k = K_c+1, \cdots, K)$.
3) Eliminate the component of noises and uncorrelated signals via (19) and (25).
4) Define a new matrix $\mathbf{r}_i^{(1)}$ and construct the new covariance matrix of coherent signals via (33).
5) Utilize root-MUSIC to resolve the DOAs of coherent signals in each subarray and find the common values of two subarrays as $\hat{\varphi}_k^r$ $(k = 1, \cdots, K_c)$.

Algorithm 2 DOA Estimation Algorithm in Coprime Planar Array

1) Calculate the covariance matrix via (6) and use Unitary-ESPRIT to solve the possible values of each subarray.
2) Find the common values of two subarrays and obtain the real DOAs as $(\hat{\varphi}_k^r, \hat{\theta}_k^r)$ $(k = K_c+1, \cdots, K)$.
3) Eliminate the component of noises and uncorrelated signals via (20) and (30).
4) Define a new matrix $\mathbf{r}_i^{(2)}$ and $\mathbf{F}_{i,m_s}$, construct $\mathbf{Y}_i$, and calculate the new covariance matrix of coherent signals as $\mathbf{R}_{\mathbf{Y}_i}^{(2)}$.
5) Utilize Unitary-ESPRIT to resolve the DOAs of coherent signals in each subarray and find the common values of two subarrays as $(\hat{\varphi}_k^r, \hat{\theta}_k^r)$ $(k = 1, \cdots, K_c)$.

IV. ANALYSIS OF MAXIMUM NUMBER OF SIGNALS RESOLVED AND COMPUTATIONAL COMPLEXITY

A. ANALYSIS OF MAXIMUM NUMBER OF SIGNALS RESOLVED

Here we analyze the maximum number of signals that can be resolved by the proposed algorithm. In coprime linear array, using the proposed algorithm to estimate the uncorrelated signals, we should meet the requirement that $K_u+P \le M_1-1$. To estimate the coherent signals, the requirement changes to $K_c \le \lceil (M_1-1)/2 \rceil$. If $P = 1$, the $K_c + K_u$ can reach the maximum value $M_1 - 2 + \lceil (M_1-1)/2 \rceil$. In conclusion, the proposed algorithm can estimate more number of signals than the number of subarray sensors when there are coherent signals.

Furthermore, in coprime planar array, when $K_u + P \le M_1^2 - 1$, we can first estimate the DOAs of uncorrelated signals. After constructing an $M_{s1} \times M_{s1}$ covariance matrix,

we can estimate maximum $K_c = M_{s1}^2 - 1$ coherent signals, while the total coherent signals are no more than M_{s2}^2, where $M_{s1} + M_{s2} - 1 = M_1$. The maximum K requires that M_{s1} and M_{s2} are big enough, and P is small enough. Thus, when $M_{s1} = \lceil (M_1+1)/2 \rceil$, $M_{s2} = M_1 + 1 - M_{s1}$, and $P = 1$, the number of resolved signals is maximum as $K = min\{M_{s2}^2, M_{s1}^2 - 1\} + M_1^2 - 2$, which can also be larger than the number of subarray sensors.

B. ANALYSIS OF COMPUTATIONAL COMPLEXITY

We analyze the computational complexity of proposed algorithm, which is divided into two parts: coprime linear array and coprime planar array.

We present an algorithm using root-MUSIC to reduce the complexity in coprime linear array. Compared with the algorithm using MUSIC, the difference of complexity between them is the complexity of subspace algorithms. The root-MUSIC costs $O\left(M_1^3 + M_2^3 + (\lceil (M_1+1)/2 \rceil)^3 + (\lceil (M_2+1)/2 \rceil)^3\right)$ while the MUSIC costs $O\left((((\lceil (M_1+1)/2 \rceil)^2 + (\lceil (M_2+1)/2 \rceil)^2) G_\varphi\right) + O\left(\left(M_1^2 + M_1^2\right)\right)$, where G_φ denotes the number of spectral points.

Similarly, the difference of complexity between the algorithm using Unitary-ESPRIT and algorithm using 2D-MUSIC is the complexity of subspace algorithms. That of former is $O\left(M_1^6 + M_2^6 + (\lceil (M_1+1)/2 \rceil)^6 + (\lceil (M_2+1)/2 \rceil)^6\right)$ and that of latter is $O\left(\left((\lceil M_1/2 \rceil)^4 + (\lceil M_2/2 \rceil)^4\right) G_\varphi G_\theta\right) + O\left(\left(M_1^4 + M_2^4\right)\right)$, where G_φ, G_θ denote the number of spectral points.

For the sake of clarity, we compare the complexities of methods in Fig. 3, where we set $M_2 = M_1 + 1$, $\Delta\theta = \Delta\varphi$, and $G_\theta = 90°/\Delta\theta + 1$, $G_\varphi = 360°/\Delta\varphi + 1$. The figure proves that root-MUSIC and Unitary-ESPRIT can truly reduce the complexity compared with spectral peak search methods. Moreover, the spectral peak search method can obtain the higher accuracy with a smaller searching step, which means costing higher complexity.

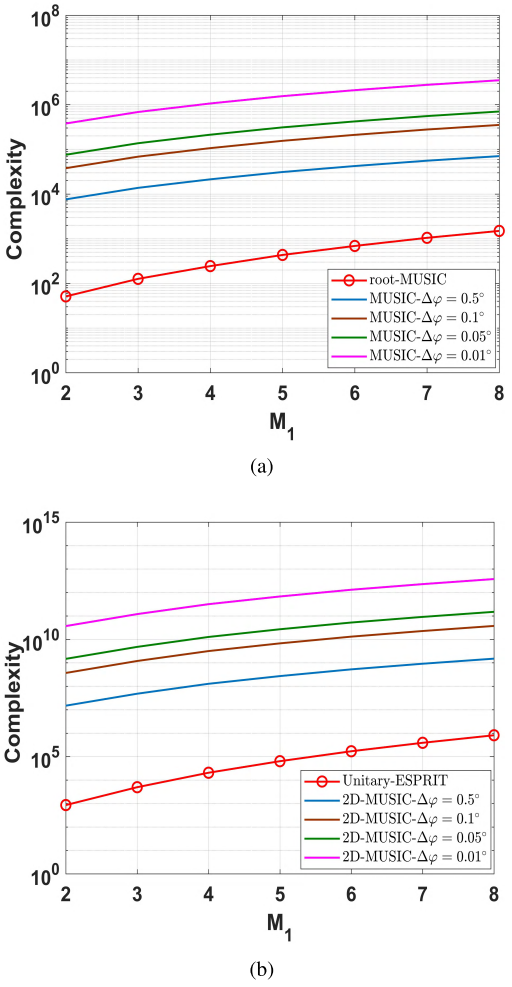

FIGURE 3. Complexity comparison versus the number of subarray sensors. (a) Coprime linear array. (b) Coprime planar array.

V. SIMULATION RESULTS

A. CRAMER-RAO BOUND OF COPRIME ARRAY

In this section, the Cramer-Rao bound (CRB) of coprime array is presented, which is plotted as a benchmark. The CRB for two-dimensional DOA estimation in planar array has been derived in [26], when uncorrelated and coherent signals coexist. Consider that a coprime planar array is also a planar array, thus, the unknown parameter vector in [26] has been changed to $\boldsymbol{\psi} = \left[\boldsymbol{\varphi}^T, \boldsymbol{\theta}^T, \boldsymbol{\beta}_r^T, \boldsymbol{\beta}_i^T\right]$, where $\boldsymbol{\varphi} = \left[\varphi_{1,1}, \cdots, \varphi_{P,L_P}, \varphi_{K_c+1}, \cdots \varphi_K\right]^T$, $\boldsymbol{\theta} = \left[\theta_{1,1}, \cdots, \theta_{P,L_P}, \theta_{K_c+1}, \cdots \theta_K\right]^T$, and $\boldsymbol{\beta}_r, \boldsymbol{\beta}_i$ are the real part and the imaginary part of the vector $\boldsymbol{\beta} = \left[\beta_{1,2}, \cdots, \beta_{1,L_1}, \beta_{2,2}, \cdots, \beta_{P,L_P}\right]^T$. We denote the mth elements in $\boldsymbol{\psi}$ as ψ_m, thus the general expression of the (m,n)th

$$\mathbf{F}_{i,m_s} = \begin{bmatrix} r_i^{(2)}\left(m_x, m_y, 1, m_s\right) & \cdots & r_i^{(2)}\left(m_x, m_y, M_{s2}, m_s\right) \\ \vdots & \cdots & \vdots \\ r_i^{(2)}\left(m_x, m_y, M_{s1}, m_s\right) & \cdots & r_i^{(2)}\left(m_x, m_y, M_{s1}+M_{s2}-1, m_s,\right) \\ \vdots & \cdots & \vdots \\ r_i^{(2)}\left(m_x, m_y, 1, M_{s1}+m_s-1,\right) & \cdots & r_i^{(2)}\left(m_x, m_y, M_{s2}, M_{s1}+m_s-1\right) \\ \vdots & \cdots & \vdots \\ r_i^{(2)}\left(m_x, m_y, M_{s1}, M_{s1}+m_s-1,\right) & \cdots & r_i^{(2)}\left(m_x, m_y, M_{s1}+M_{s2}-1, M_{s1}+m_s-1\right) \end{bmatrix} \tag{34}$$

element in Fisher information matrix (FIM) can be expressed as

$$FIM_{\psi_m\psi_n} = -E\left[\frac{\partial^2 L}{\partial\psi_m\partial\psi_n}\right]. \tag{36}$$

Moreover, the FIMs corresponding to each vector included in $\boldsymbol{\psi}$ are denoted as $\mathbf{FIM}_{\varphi\varphi}$, $\mathbf{FIM}_{\theta\theta}$, $\mathbf{FIM}_{\beta_r\beta_r}$, and $\mathbf{FIM}_{\beta_i\beta_i}$, respectively, and to the cross terms between each vector are $\mathbf{FIM}_{\varphi\theta}$, $\mathbf{FIM}_{\varphi\beta_r}$, $\mathbf{FIM}_{\varphi\beta_i}$, $\mathbf{FIM}_{\theta\varphi}$, $\mathbf{FIM}_{\theta\beta_r}$, $\mathbf{FIM}_{\theta\beta_i}$, $\mathbf{FIM}_{\beta_r\varphi}$, $\mathbf{FIM}_{\beta_r\theta}$, $\mathbf{FIM}_{\beta_r\beta_i}$, $\mathbf{FIM}_{\beta_i\varphi}$, $\mathbf{FIM}_{\beta_i\theta}$ and $\mathbf{FIM}_{\beta_i\beta_r}$. As a result, the whole FIM is given as

$$\mathbf{FIM}_{\psi\psi} = \begin{bmatrix} \mathbf{FIM}_{\varphi\varphi} & \mathbf{FIM}_{\varphi\theta} & \mathbf{FIM}_{\varphi\beta_r} & \mathbf{FIM}_{\varphi\beta_i} \\ \mathbf{FIM}_{\theta\varphi} & \mathbf{FIM}_{\theta\theta} & \mathbf{FIM}_{\theta\beta_r} & \mathbf{FIM}_{\theta\beta_i} \\ \mathbf{FIM}_{\beta_r\varphi} & \mathbf{FIM}_{\beta_r\theta} & \mathbf{FIM}_{\beta_r\beta_r} & \mathbf{FIM}_{\beta_r\beta_i} \\ \mathbf{FIM}_{\beta_i\varphi} & \mathbf{FIM}_{\beta_i\theta} & \mathbf{FIM}_{\beta_i\beta_r} & \mathbf{FIM}_{\beta_i\beta_i} \end{bmatrix}. \tag{37}$$

Define $\mathbf{H} = \mathbf{FIM}_{\psi\psi}^{-1}$, and we can obtain the CRBs of azimuth angle and coherent angle, respectively, as

$$CRB_{\varphi} = \sqrt{\frac{1}{K}\sum_{k=1}^{K} H_{kk}}, \tag{38}$$

$$CRB_{\theta} = \sqrt{\frac{1}{K}\sum_{k=K+1}^{2K} H_{kk}}, \tag{39}$$

where $H_{k,k}$ denotes the (k,k)th element of $\mathbf{H}$.

We can consider the linear array as a special planar array, where only the azimuth can be solved. Hence, we just need change $\boldsymbol{\psi} = \left[\boldsymbol{\varphi}^T, \boldsymbol{\beta}_r^T, \boldsymbol{\beta}_i^T\right]$, and the FIM and CRB of azimuth angle are respectively given by

$$\mathbf{FIM}_{\psi\psi} = \begin{bmatrix} \mathbf{FIM}_{\varphi\varphi} & \mathbf{FIM}_{\varphi\beta_r} & \mathbf{FIM}_{\varphi\beta_i} \\ \mathbf{FIM}_{\beta_r\varphi} & \mathbf{FIM}_{\beta_r\beta_r} & \mathbf{FIM}_{\beta_r\beta_i} \\ \mathbf{FIM}_{\beta_i\varphi} & \mathbf{FIM}_{\beta_i\beta_r} & \mathbf{FIM}_{\beta_i\beta_i} \end{bmatrix}. \tag{40}$$

$$CRB_{\varphi} = \sqrt{\frac{1}{K}\sum_{k=1}^{K} H_{kk}}. \tag{41}$$

B. SIMULATION EXPERIMENTS

To measure the accuracy of the algorithms, we define the root mean square error (RMSE) as

$$\mathrm{RMSE} = \sqrt{\frac{1}{QK}\sum_{q=1}^{Q}\left\|\boldsymbol{\xi} - \hat{\boldsymbol{\xi}}_q\right\|^2}. \tag{42}$$

where Q, $\boldsymbol{\xi}$ and $\hat{\boldsymbol{\xi}}_q$ are the number of Monte Carlo simulations, the real values and the qth estimated values, respectively.

1) DOA ESTIMATION OF TWO DISTINCT SIGNALS FROM THE SAME ANGLE

There are two possible situations when two distinct sources from the same azimuth (for simplicity we only consider coprime linear array here). One situation is that one of the coherent signals and one uncorrelated signal come from the same azimuth. The other is that the two signals, from the same azimuth, are both uncorrelated signals or belong to the groups of coherent signal. With the proposed algorithm, we can separate two signals in different steps in the former situation. But we cannot obtain the results in the latter situation because their peaks are totally overlapped in spatial spectrum in the same estimating step.

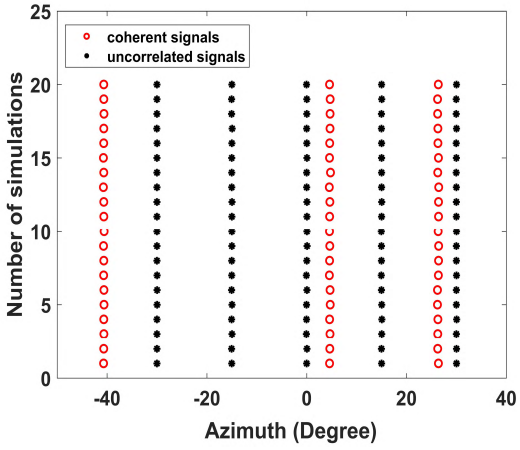

(a)

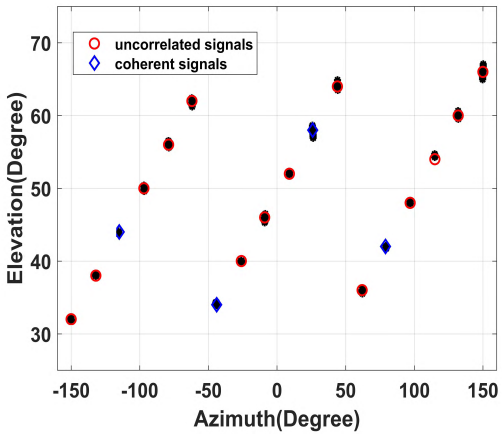

(b)

FIGURE 4. Distribution of estimated values. (a) Coprime linear array. (b) Coprime planar array.

Hence, we assume that there are two coherent signals at $\varphi_{1,1} = 0.7°$ and $\varphi_{1,2} = 25.8°$, and one signal uncorrelated to the other two signals at $\varphi_3 = 0.7°$ with a signal-to-noise ratio (SNR) of 15dB and $J = 500$. We set $M_1 = 7$ and $M_2 = 9$. The results of proposed algorithm are listed in Table 1. Through finding the nearest values between sets of two subarrays, we can ensure that $\hat{\varphi}_{1,1} = 0.6979°$, $\hat{\varphi}_{1,2} = 25.82°$ and $\hat{\varphi}_3 = 0.6993°$.

Both conclusions of two situations can be applied to coprime planar array, where the two signals come from the same azimuth and elevation angle. The signals are from $(\varphi_{1,1}, \theta_{1,1}) = (45°, 45°)$, $(\varphi_{1,2}, \theta_{1,2}) = (64°, 54°)$, and $(\varphi_3, \theta_3) = (45°, 45°)$, and $M_1 = 4$, $M_2 = 5$. The estimated values are shown in Table 2. Obviously, $(\hat{\mu}_1^r, \hat{\nu}_1^r) = (0.5002, 0.5001)$, $(\hat{\mu}_2^r, \hat{\nu}_2^r) = (0.3545, 0.7271)$,

TABLE 1. The detailed values of results in coprime linear array.

Value	Subarray 1	Subarray 2
$\Phi_{i,3}^{(1)}$	-61.2275° -40.8677° -25.6005° -12.1148° 0.7077° 13.5665° 27.1805° 42.7670° 64.3216°	-57.6654° -34.0022° -15.8732° 0.6993° 17.3326° 35.7065° 60.3829°
$\Phi_{i,1}^{(1)}$	61.5859° 41.0950° 25.7908° 12.2903° -0.5361° -13.3901° -26.9879° -42.5337° -63.9285°	46.1586° 25.8200° 8.6172° -7.8097° -24.9355° -45.0166° -83.2292°
$\Phi_{i,2}^{(1)}$	64.3349° 42.7748° 27.1870° 13.5724° 0.7135° -12.1089° -25.5941° -40.8601° -61.2155°	60.3801° 35.7048° 17.3312° 0.6979° -15.8747° -34.0038° -57.6679°

TABLE 2. The detailed values of results in coprime planar array.

Value	Subarray 1	Subarray 2
$\Phi_{i,3}^{(2)}$	-0.6996 -0.2996 0.1004 0.5004 0.9004	-0.9998 -0.4998 0.0002 0.5002
$\Theta_{i,3}^{(2)}$	-0.7001 -0.3001 0.0999 0.4999 0.8999	-0.5002 -0.0002 0.4998 0.9998
$\Phi_{i,1}^{(2)}$	-0.6998 -0.2998 0.1002 0.5002 0.9002	-0.9998 -0.4998 0.0002 0.5002
$\Theta_{i,1}^{(2)}$	-0.7000 -0.3000 0.1000 0.5000 0.9000	-0.9999 -0.4999 0.0001 0.5001
$\Phi_{i,2}^{(2)}$	-0.8456 -0.4456 -0.0456 0.3544 0.7544	-0.6455 -0.1455 0.3545 0.8545
$\Theta_{i,2}^{(2)}$	-0.8726 -0.4726 -0.0726 0.3274 0.7274	-0.7729 -0.2729 0.2271 0.7271

and $(\hat{\mu}_3^r, \hat{v}_3^r) = (0.5002, 0.4998)$, and then $(\hat{\theta}_{1,1}, \hat{\varphi}_{1,1}) = (44.967^\circ, 45.007^\circ)$, $(\hat{\theta}_{1,2}, \hat{\varphi}_{1,2}) = (64.016^\circ, 54.007^\circ)$, and $(\hat{\theta}_3, \hat{\varphi}_3) = (44.997^\circ, 45.009^\circ)$.

In conclusion, the proposed algorithm is valid to estimate the DOAs, even if there are two distinct signals from the same angle, where one is an uncorrelated signal and the other belongs to a group of coherent signals.

2) FEASIBILITY DEMONSTRATION WHEN THE NUMBER OF SIGNALS IS BIGGER THAN THAT OF SUBARRAY SENSORS

In the second simulation, we consider the case of $K_u = 5$, $P = 1$ and $K_c = 3$ with a SNR of 15dB in coprime linear array, where $M_1 = 7$ and $M_2 = 9$. Next, we conduct the simulation in coprime planar array where $M_1 = 4$ and $M_2 = 5$. We set $K_u = 14$, $P = 1$, and $K_c = 4$ with a SNR of 15dB. The estimated values of 20 times Monte Carlo simulations are shown in Fig. 4 (a) and (b). The figure shows that the proposed algorithms can realize the estimation of the true DOAs, when there is the coexistence of both uncorrelated and coherent signals, under the condition that the number of signals is bigger than that of subarray sensors.

3) RMSE COMPARISON UNDER DIFFERENT SNRs

In the third simulation, we compare the RMSE of proposed algorithm using root-MUSIC with that of algorithm using MUSIC and FCM under SNRs from -5dB to 15dB at 5dB intervals and $J = 500$, where $M_1 = 7$ and $M_2 = 9$. There are two coherent signals at $\varphi_{1,1} = -40.6^\circ$ and $\varphi_{1,2} = 25.8^\circ$, and one signal uncorrelated to the other two at $\varphi_3 = 0.2^\circ$. Furthermore, we compare the proposed algorithm using Unitary-ESPRIT with the algorithm using 2D-MUSIC, where $M_1 = 4$ and $M_2 = 5$. Assume that two coherent signals come from $(\varphi_{1,1}, \theta_{1,1}) = (25.3^\circ, 28.1^\circ)$ and $(\varphi_{1,2}, \theta_{1,2}) = (64.4^\circ, 54.2^\circ)$, and one uncorrelated signal comes from $(\varphi_3, \theta_3) = (45.2^\circ, 45.7^\circ)$. We conduct 100 simulations for each SNR and vary searching step in the range from 0.5°, 0.1°, and 0.01°.The results are shown in Fig. 5 and Fig. 6, respectively.

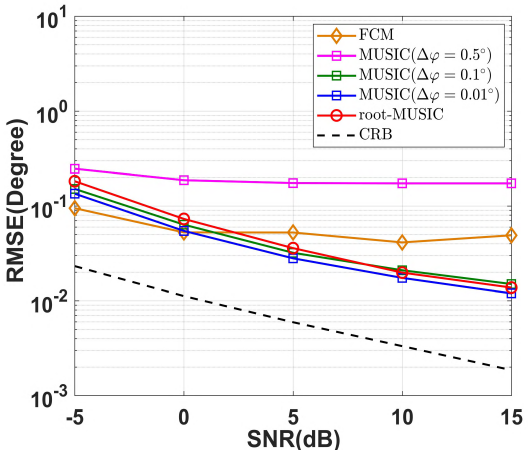

FIGURE 5. RMSE versus SNR in coprime linear array.

The Fig. 5 demonstrates that FCM is not sensitive to SNR. Because there exists the fence effect in spatial spectrum and the real angles are not located at the searching grid, the accuracy of MUSIC with $\Delta\varphi = 0.5^\circ$ do not improve when SNR is high. Moreover, the smaller searching step can acquire higher accuracy. Hence, the RMSE of MUSIC with $\Delta\varphi = 0.01^\circ$ is smaller than that of MUSIC with $\Delta\varphi = 0.1^\circ$, but the gap between them is not big. In low SNR, the RMSE of FCM is lowest, while that of root-MUSIC is highest. However, when SNR is high, root-MUSIC has close accuracy as MUSIC with small searching steps, and higher accuracy than FCM. Although the RMSE of MUSIC with $\Delta\varphi = 0.01^\circ$ is closest to the CRB, considering the complexity, root-MUSIC is more computationally efficient than MUSIC.

As for coprime planar array, the RMSE of 2D-MUSIC with $\Delta\varphi = 0.5^\circ$ is highest due to fence effect. The proposed algorithm using Unitary-ESPRIT obtains higher RMSE than 2D-MUSIC with small searching steps in low SNR, but the

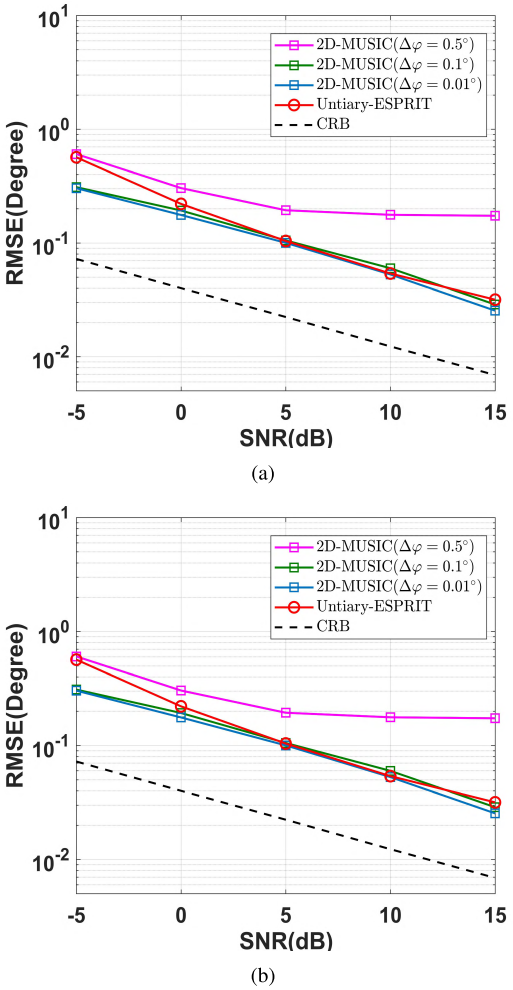

FIGURE 6. RMSE versus SNR in coprime planar array. (a) Elevation. (b) Azimuth.

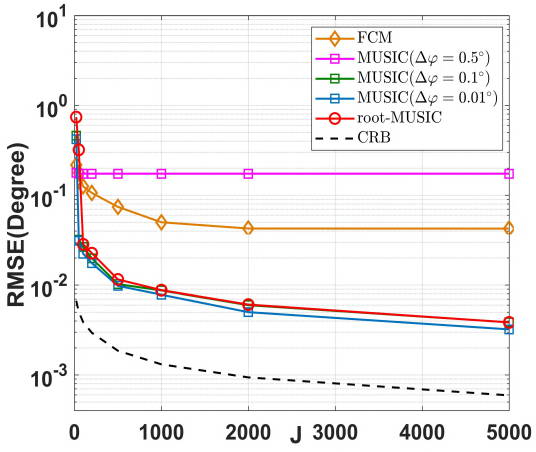

FIGURE 7. RMSE versus J in coprime linear array.

gap between them becomes smaller with SNR increasing. They have the close RMSE in high SNR. Also given the complexity, even though the 2D-MUSIC with $\Delta\varphi = 0.01°$ is closest to the CRB, the Unitary-ESPRIT is more favorable because it costs much lower complexity to acquire the highly precise estimated values.

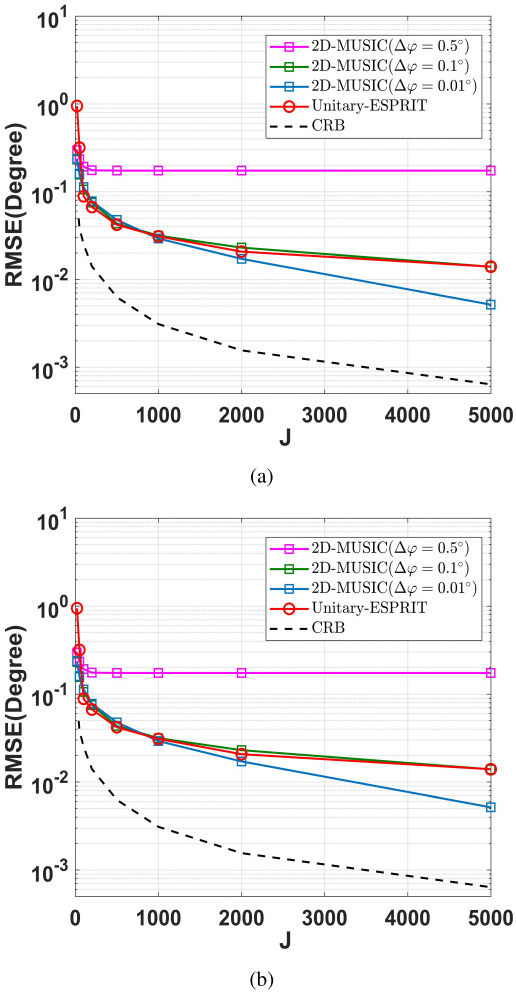

FIGURE 8. RMSE versus J in coprime planar array. (a) Azimuth. (b) Elevation.

4) RMSE COMPARISON UNDER THE DIFFERENT NUMBER OF SNAPSHOTS

Consider situations used in simulation 3 again. The number of snapshots is varied in the range from $J = [20, 50, 100, 200, 500, 1000, 2000, 5000]$, when SNR $= 15$dB, and the results are shown in Fig. 7 and Fig. 8, respectively. With the increase of number of snapshots, the accuracy of the proposed algorithms becomes higher. Moreover, the decline gradually reaches a plateau. The figures also prove the conclusions in simulation 3.

VI. CONCLUSIONS

The paper has presented the DOA estimation algorithm in coprime array when there is the coexistence of both coherent and uncorrelated signals. The paper has described coprime linear array model for 1D DOA estimation and coprime planar array model for 2D DOA estimation. We then present the associated algorithms, analyze the computational complexity and the maximum number of signals resolved, and conduct the simulation experiments, respectively. We prove that both

proposed algorithms in two models can estimate signals of which the number is bigger than that of subarray sensors, when there exist the coherent signals. And compared with spectral peak search method, the root-MUSIC in coprime linear array and Unitary-ESPRIT in coprime planar array have greatly reduced the complexity. They obtain the higher RMSE in low SNR than spectral peak search methods, while they can obtain the close accuracy when SNR is high. Moreover, the proposed method can separate two signals coming from the same angle, when one of them is a uncorrelated signal and the other belongs to a group of coherent signals.

APPENDIX
PROOF OF THEOREM 1

The $\mathbf{F}_{i,m_s}$ in (34) can be reformulated as

$$\mathbf{F}_{i,m_s} = \mathbf{B}_{c_i}\mathbf{D}_{y_i}^{m_s-1}\left[\boldsymbol{\zeta}\ \mathbf{D}_{x_i}\boldsymbol{\zeta}\ \cdots\ \mathbf{D}_{x_i}^{M_{s2}-1}\boldsymbol{\zeta}\right], \tag{43}$$

where $\boldsymbol{\zeta} = [\sigma_1^2\zeta_{1,1}^{m_x,m_y}, \cdots, \sigma_P^2\zeta_{P,L_P}^{m_x,m_y}]$, and

$$\begin{aligned}\mathbf{D}_{x_i} &= \begin{bmatrix} d_{x_{1,1}} & & \\ & \ddots & \\ & & d_{x_{P,L_P}} \end{bmatrix} \\ &= \begin{bmatrix} e^{-j\pi M_{\tilde{i}}\sin\theta_{1,1}\cos\varphi_{1,1}} & & \\ & \ddots & \\ & & e^{-j\pi M_{\tilde{i}}\sin\theta_{P,L_P}\cos\varphi_{P,L_P}} \end{bmatrix},\end{aligned} \tag{44}$$

$$\begin{aligned}\mathbf{D}_{y_i} &= \begin{bmatrix} d_{y_{1,1}} & & \\ & \ddots & \\ & & d_{y_{P,L_P}} \end{bmatrix} \\ &= \begin{bmatrix} e^{-j\pi M_{\tilde{i}}\sin\theta_{1,1}\sin\varphi_{1,1}} & & \\ & \ddots & \\ & & e^{-j\pi M_{\tilde{i}}\sin\theta_{P,L_P}\sin\varphi_{P,L_P}} \end{bmatrix}.\end{aligned} \tag{45}$$

$\mathbf{B}_{c_i}$ is denoted as $\mathbf{B}_{c_i} = [\tilde{\mathbf{a}}_{y_i}^*(\varphi_{1,1},\theta_{1,1})\otimes\tilde{\mathbf{a}}_{x_i}^*(\varphi_{1,1},\theta_{1,1}), \cdots, \tilde{\mathbf{a}}_{y_i}^*(\varphi_{P,L_P},\theta_{P,L_P})\otimes\tilde{\mathbf{a}}_{x_i}^*(\varphi_{P,L_P},\theta_{P,L_P})]$, where $\tilde{\mathbf{a}}_{x_i} = \tilde{\mathbf{J}}\mathbf{a}_{x_i}$, $\tilde{\mathbf{a}}_{y_i} = \tilde{\mathbf{J}}\mathbf{a}_{y_i}$, and $\tilde{\mathbf{J}} = [\mathbf{I}_{M_{s1}}, \mathbf{0}_{M_{s1},M-M_{s1}}]$. Thus,

$$\mathbf{F}_{i,m_s} = \mathbf{B}_{c_i}\mathbf{D}_{y_i}\Sigma^{(2)}\begin{bmatrix} 1 & d_{x_{1,1}} & \cdots & d_{x_{1,1}}^{M_{s2}-1} \\ \vdots & \vdots & \vdots & \vdots \\ 1 & d_{x_{P,L_p}} & \cdots & d_{x_{P,L_P}}^{M_{s2}-1} \end{bmatrix}, \tag{46}$$

where $\boldsymbol{\Sigma}^{(2)} = diag(\boldsymbol{\zeta})$. Next, $\mathbf{F}_i$ can be rewritten as

$$\mathbf{F}_i = \mathbf{B}_{c_i}\boldsymbol{\Sigma}^{(2)}\mathbf{D}_i, \tag{47}$$

where $\mathbf{D}_i = [\mathbf{d}_{y_{1,1}}\otimes\mathbf{d}_{x_{1,1}}, \cdots, \mathbf{d}_{y_{P,L_P}}\otimes\mathbf{d}_{x_{P,L_P}}]$, $\mathbf{d}_{x_{p,\ell}} = [1, \cdots, d_{x_{p,\ell}}^{M_{s2}-1}]^T$, and $\mathbf{d}_{y_{p,\ell}} = [1, \cdots, d_{y_{p,\ell}}^{M_{s2}-1}]^T$. At last, the covariance matrix of coherent signals is given by

$$\mathbf{R}_{\mathbf{Y}_i}^{(2)} = \mathbf{F}_i\mathbf{F}_i^H = \mathbf{B}_{c_i}\Sigma^{(2)}\mathbf{D}_i\mathbf{D}_i^H\Sigma^{(2)H}\mathbf{B}_{c_i}^H. \tag{48}$$

Given the conclusion in [12], we can find that $\mathbf{B}_{c_i}$ is of full column rank when $M_{s1}^2 > K_c$, $\Sigma^{(2)}$ is of full rank, and $\mathbf{D}_i\mathbf{D}_i^H$ is of full of rank when $M_{s2}^2 \geq K_c$. Thus, the rank of $\mathbf{R}_{\mathbf{Y}_i}^{(2)}$ is K_c, which satisfies the requirement of using subspace algorithms. This completes the proof of Theorem 1.

REFERENCES

[1] J. E. Ball and N. H. Younan, "Radar and radio signal processing," *Electronics*, vol. 6, no. 3, p. 64, 2017.
[2] Y. Wang, S. Ma, G. L. Liang, and Z. Fan, "Chirp spread spectrum of orthogonal frequency division multiplexing underwater acoustic communication system based on multi-path diversity receive," *Acta Phys. Sinca*, vol. 63, no. 4, p. 044302, 2014.
[3] Y. Zhou, Y. Wu, D. Chen, and F. Tong, "Compressed sensing estimation of underwater acoustic MIMO channels based on temporal joint sparse recovery," *J. Electron. Inf. Technol.*, vol. 38, no. 3, pp. 1920–1927, 2016.
[4] A. Gaber and A. Omar, "Sub-nanosecond accuracy of TDOA estimation using matrix pencil algorithms and IEEE 802.11," in *Proc. IEEE. Int. Symp. Wireless Commun. Syst.*, Aug. 2012, pp. 646–650.
[5] P. Heidenreich, A. M. Zoubir, and M. Rubsamen, "Joint 2-D DOA estimation and phase calibration for uniform rectangular arrays," *IEEE Trans. Signal Process.*, vol. 60, no. 9, pp. 4683–4693, Sep. 2012.
[6] R. O. Schmidt, "Multiple emitter location and signal parameter estimation," *IEEE Trans. Antennas Propag.*, vol. 34, no. 3, pp. 276–280, Mar. 1986.
[7] D. Zhang, Y. S. Zhang, G. M. Zheng, C. Q. Feng, and J. Tang, "Improved DOA estimation algorithm for co-prime linear arrays using root-MUSIC algorithm," *Electron. Lett.*, vol. 53, no. 18, pp. 1277–1279, Sep. 2017.
[8] C. Zhou and J. Zhou, "Direction-of-arrival estimation with coarray ESPRIT for coprime array," *Sensors*, vol. 17, no. 8, p. 1779, 2017.
[9] B. Byun and D. Yoo, "Improved direction of arrival estimation based on coprime array and propagator method by noise power spectral density estimation," *J. Adv. Navigat. Tech.*, vol. 20, pp. 367–373, 2016.
[10] M. D. Zoltowski, M. Haardt, and C. P. Mathews, "Closed-form 2-D angle estimation with rectangular arrays in element space or beamspace via unitary ESPRIT," *IEEE Trans. Signal Process.*, vol. 44, no. 2, pp. 316–328, Feb. 1996.
[11] M. Haardt and J. A. Nossek, "Unitary ESPRIT: How to obtain increased estimation accuracy with a reduced computational burden," *IEEE Trans. Signal Process.*, vol. 43, no. 5, pp. 1232–1242, May 1995.
[12] T.-J. Shan, M. Wax, and T. Kailath, "On spatial smoothing for direction-of-arrival estimation of coherent signals," *IEEE Trans. Acoust., Speech, Signal Process.*, vol. ASSP-33, no. 4, pp. 806–811, Apr. 1985.
[13] C.-C. Yeh, J.-J. Lee, and Y.-Y. Chen, "Estimating two-dimensional angles of arrival in coherent source environment," *IEEE Trans. Acoust., Speech Signal Process.*, vol. 37, no. 1, pp. 153–155, Jan. 1989.
[14] F.-M. Han and X.-D. Zhang, "An ESPRIT-like algorithm for coherent DOA estimation," *IEEE Antennas Wireless Propag. Lett.*, vol. 4, no. 12, pp. 443–446, Dec. 2005.
[15] X. Xu, Z. Ye, Y. Zhang, and C. Chang, "A deflation approach to direction of arrival estimation for symmetric uniform linear array," *IEEE Antennas Wireless Propag. Lett.*, vol. 5, no. 1, pp. 486–489, 2006.
[16] Z. Ye and X. Xu, "DOA estimation by exploiting the symmetric configuration of uniform linear array," *IEEE Trans. Antennas Propag.*, vol. 55, no. 12, pp. 3716–3720, Dec. 2007.
[17] X. Xu and Z. Ye, "Two-dimensional direction of arrival estimation by exploiting the symmetric configuration of uniform rectangular array," *IET Radar, Sonar Navigat.*, vol. 6, no. 5, pp. 307–313, Jun. 2012.
[18] P. Pal and P. P. Vaidyanathan, "Coprime sampling and the music algorithm," in *Proc. IEEE Digit. Signal Process. Workshop, IEEE Signal Process. Educ. Workshop*, Sedona, AZ, USA, Jan. 2011, pp. 289–294.
[19] P. P. Vaidyanathan and P. Pal, "Sparse sensing with co-prime samplers and arrays," *IEEE Trans. Signal Process.*, vol. 59, no. 2, pp. 573–586, Feb. 2011.
[20] C. Zhou, Z. Shi, Y. Gu, and X. Shen, "DECOM: DOA estimation with combined MUSIC for coprime array," in *Proc. IEEE Int. Conf. Wireless Commun. Signal Process. (WCSP)*, Oct. 2013, pp. 1–5.
[21] Q. Wu, F. Sun, P. Lan, G. Ding, and X. Zhang, "Two-dimensional direction-of-arrival estimation for co-prime planar arrays: A partial spectral search approach," *IEEE Sensors J.*, vol. 16, no. 14, pp. 5660–5670, Jul. 2016.
[22] W. Zheng, X. Zhang, and H. Zhai, "Generalized coprime planar array geometry for 2-D DOA estimation," *IEEE Commun. Lett.*, vol. 21, no. 5, pp. 1075–1078, May 2017.

[23] S. Qin, Y. D. Zhang, and M. G. Amin, "DOA estimation of mixed coherent and uncorrelated targets exploiting coprime MIMO radar," *Digit. Signal Process.*, vol. 61, pp. 26–34, Feb. 2017.
[24] E. BouDaher, F. Ahmad, and M. G. Amin, "Sparsity-based direction finding of coherent and uncorrelated targets using active nonuniform arrays," *IEEE Signal Process. Lett.*, vol. 22, no. 10, pp. 1628–1632, Oct. 2015.
[25] Y. Hu, Y. Liu, and X. Wang, "DOA estimation of coherent signals on coprime arrays exploiting fourth-order cumulants," *Sensors*, vol. 17, no. 4, p. 682, 2017.
[26] Y. Zhang *et al.*, "Estimation of two-dimensional direction-of-arrival for uncorrelated and coherent signals with low complexity," *IET Radar Sonar Navigat.*, vol. 4, no. 4, pp. 507–519, 2010.

HAIYUN XU received the B.S. degree from the National Digital Switching System Engineering and Technological Research Center (NDSC), Zhengzhou, China, in 2016, where he is currently pursuing the M.S. degree in communications and information system. His main research interests include wireless communication theory, signal processing, and parameter estimation.

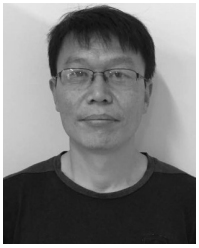

DAMING WANG was born in 1971. He is currently a Professor with the National Digital Switching System Engineering and Technological Research Center, Zhengzhou, China. His main research interests include wireless communication theory, satellite and mobile communication, and signal processing.

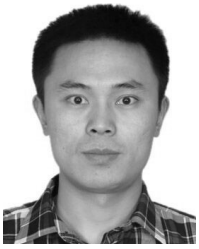

BIN BA received the M.S. and Ph.D. degrees from the National Digital Switching System Engineering and Technological Research Center, Zhengzhou, China, in 2012 and 2015, respectively, where he is currently working in communications and information system. His main research interests include wireless communication theory, signal processing, and parameter estimation.

WEIJIA CUI received the M.S. and Ph.D. degrees from the National Digital Switching System Engineering and Technological Research Center, Zhengzhou, China, in 2001 and 2007, respectively, where he is currently working in communications and information system. His main research interests include wireless communication theory, satellite and mobile communication, and signal processing.

YANKUI ZHANG received the M.S. degree from the National Digital Switching System Engineering and Technological Research Center, Zhengzhou, China, in 2016, where he is currently pursuing the Ph.D. degree in communications and information system. His main research interests include array signal processing and parameter estimation.